


## COMPARISON OF DROUGHT INDICES FOR EVALUATING AGRICULTURAL DROUGHT RISK IN HIGHLAND REGIONS

Teerawong LAOSUWAN<sup>1,4</sup>, Yannawut UTTARUK<sup>2</sup>, Phaisarn JEEFOO<sup>3</sup>,  
Jumpol ITSARAWISUT<sup>1,4\*</sup>

DOI: 10.21163/GT\_2024.192.12

### ABSTRACT

The impact of drought on human livelihoods is significant, as it is a natural disaster that affects various aspects of life. This research aims to evaluate suitable drought indices for assessing agricultural drought risk in highland regions, focusing on the Nan Watershed in Northern Thailand. The study analyzed three types of drought indices: Normalized Monthly Precipitation Anomaly Percentage (NPA), Vegetation Health Index (VHI), and Normalized Vegetation Supply Water Index (NVSWI). Rainfall data from the Tropical Rainfall Measuring Mission (TRMM) TRMM 3B42 product was used to assess the suitability of these indices for evaluating agricultural drought risk over a ten-year period (2013-2022). The study found that ground-based rainfall data and TRMM3B42 satellite data have a very high statistical correlation, with a correlation coefficient of 0.8945. Analyzing the statistical correlation of suitable drought indices for assessing agricultural drought risk revealed that NVSWI had the highest statistical correlation with a coefficient of 0.956. VHI had a correlation coefficient of -0.8179, and NPA had a correlation coefficient of 0.867. For evaluating the suitability of drought indices affecting the assessment of agricultural drought risk in high areas, focusing on the Nan Watershed in Northern Thailand, this study concludes that NVSWI is the most suitable index for assessing agricultural drought risk in high areas.

**Key-words:** Remote Sensing, Drought Indices, NPA, VHI, NVSWI, TRMM

### 1. INTRODUCTION

Drought is a natural disaster that significantly impacts human livelihoods by causing dry conditions and a noticeable decline in quality of life (Rotjanakusol & Laosuwan, 2018; Rotjanakusol & Laosuwan, 2019). It is a phenomenon that takes time to reveal its effects (Uttarak & Laosuwan, 2019), which can persist for extended periods as drought encroaches slowly. This contrasts with phenomena like floods, where impacts are immediately evident through rising water levels (Lloyd-Hughes & Saunders, 2002; Wang et al., 2020). Several factors contribute to drought, such as lower-than-normal rainfall (drought), uneven distribution of rainfall, prolonged dry spells, low soil water retention, insufficient water storage capacity, and the silting up of existing water sources leading to runoff into major rivers and ultimately the sea (Nanzad et al., 2019; Chen et al., 2020). These causes result in varied impacts depending on the nature of the affected area and the specific causes of drought in that area (Cui et al., 2021; Iamampai et al., 2023).

---

<sup>1</sup>Department of Physics, Faculty of Science, Mahasarakham University, Maha Sarakham, Thailand, [teerawong@msu.ac.th](mailto:teerawong@msu.ac.th), [jumpol.s@msu.ac.th](mailto:jumpol.s@msu.ac.th)

<sup>2</sup>Department of Biology, Faculty of Science, Mahasarakham University, Maha Sarakham, Thailand, [yannawut.u@msu.ac.th](mailto:yannawut.u@msu.ac.th)

<sup>3</sup>Geographic Information Science Field of Study, School of Information and Communication Technology, University of Phayao, Phayao, Thailand, [phaisarn.je@up.ac.th](mailto:phaisarn.je@up.ac.th)

<sup>4</sup>Space Technology and Geo-Informatics Research Unit, Faculty of Science, Mahasarakham University, Maha Sarakham, Thailand

\*Corresponding author: [jumpol.s@msu.ac.th](mailto:jumpol.s@msu.ac.th)

Drought has different meanings (Prabnakorn et al., 2018). Generally, it refers to periods of significantly lower-than-average rainfall and is considered a permanent feature of regional climates, such as deserts with annual rainfall below 100 mm. In contrast, temporary droughts feature lower-than-normal precipitation, influenced by climatic variability such as higher temperatures, lower humidity, and strong winds (Magyari-Saska & Haidu 2009; Haidu & Magyari-Saska, 2010; Raksapatcharawong et al., 2020). Drought lacks a precise definition and can occur in any region of the world. Simply put, it means no rain in a particular area for an extended period, inhibiting plant and life growth (Fussel & Klein, 2006; Hannaford, 2018). Arid conditions exist on every continent, with local life adapting to these environments or maintaining natural balances, such as in African deserts (Muyambo et al., 2017). Drought can also occur anywhere, with severity depending on various factors, including physical, ecological, and human activities (Kamanga et al., 2020). Drought characteristics can be classified in several ways, with different definitions as follows: 1) meteorological drought, referring to low rainfall in the studied area; 2) agricultural drought, describing insufficient soil moisture for crops due to low rainfall; 3) hydrological drought, concerning low reserves of surface and groundwater; and 4) socioeconomic drought, which considers resource availability and demand, leading to scarcity when demand exceeds supply. This last type focuses on human needs and resource limitations (Copernicus, 2020). Agricultural drought specifically concerns inadequate water supply for agriculture due to insufficient rainfall or prolonged dry spells during critical growth periods or high evapotranspiration rates, resulting in soil moisture deficits (Wongtui & Nilsonthi, 2024).

Satellite remote sensing has demonstrated its effectiveness as a valuable and dependable tool for monitoring drought conditions (Rotjanakusol & Laosuwan, 2020; Meena & Laosuwan; 2021; Laosuwan et al., 2022; Itsarawisut et al., 2024). Additionally, it excels in analyzing the progression of drought over temporal and spatial (Nakapan & Hongthong, 2022; Yu et al., 2022; Hongthong & Nakapan, 2023). Satellite remote sensing for operational drought monitoring has mainly relied on the use of Normalized Difference Vegetation Index (NDVI) data from the National Oceanic and Atmospheric Administration (NOAA) Advanced Very High Resolution Radiometer (AVHRR). The NDVI, created in the early 1970s by Rouse et al. (1974), is a straightforward mathematical transformation of data from two commonly available spectral bands on most satellite-based sensors, the visible red and near infrared (NIR). AVHRR NDVI-based metrics have been utilized for monitoring drought for over two decades, with roots in the pioneering studies of Tucker et al., (1986), Kogan (1990), Burgan et al., (1996), Unganai and Kogan (1998). Drought indices are metrics indicating the dryness of an area based on influential factors such as agricultural land (Liu et al., 2023; Li et al., 2024; Wu et al., 2024). These indices have been developed and refined using various variables (Zargar et al., 2011; Zhou et al., 2021). Additionally, the application of satellite data products enhances the accuracy of drought assessments, as evidenced by research in multiple countries utilizing remote sensing technology for this purpose (Ndayiragije & Li, 2022). According to the Office of Water Resources (Region 9), the Nan Watershed is a major watershed in Northern Thailand, covering parts of Nan, Uttaradit, Phitsanulok, Phichit, and Nakhon Sawan provinces. This basin continues to experience recurrent drought (Ministry of Natural Resources and Environment, 2011). This research aims to evaluate appropriate drought indices for assessing agricultural drought risk in highland regions, focusing on the Nan Watershed in Northern Thailand.

## 2. MATERIALS AND METHODS

### 2.1. Study Area

The Nan Watershed (**Fig.1**) is located in Northern Thailand, covering a total area of 34,682.04 km<sup>2</sup>. The basin extends in a north-south direction, situated between latitudes 15° 42' N and 18° 37' N and longitudes 99° 51' E and 101° 21' E. The topography of the Nan Watershed is predominantly mountainous, influenced by the southwest and northeast monsoons.

Additionally, occasional depressions and typhoons from the South China Sea pass through, resulting in distinct seasons: the rainy season from May to October, the winter from late October to February, and the summer from March to April. The basin has an average annual temperature of 26.3°C, with the highest average temperature of 36.6°C recorded in April and the lowest average temperature of 15.3°C in December. The monthly average temperature ranges from 22.1°C to 29.3°C. The average annual rainfall is 1,371.0 mm, with monthly averages ranging from 5.9 mm to 280.9 mm.

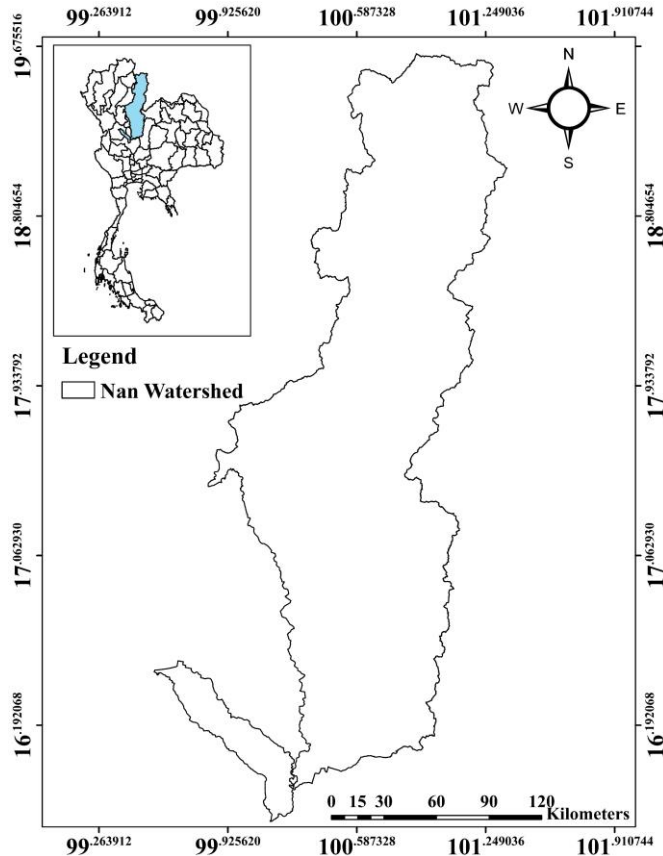


Fig. 1. Nan Watershed.

## 2.2. Data Acquisition and Pre-processing

### 2.2.1. MODIS NDVI and LST Products

The NDVI and LST products from MODIS (MOD13C2 and MOD11C3, respectively) for the period 2012-2022 were used in this study. Both products were downloaded from the website <https://ladsweb.modaps.eosdis.nasa.gov/>, the quality of the MOD13C2 satellite data was transform the NDVI values into real values by multiplying the fixed pixel values with a scaling factor of 0.0001, and the MOD11C3 data was Calculate the actual value by multiplying the pixel value by 0.02, then subtracting 273.15 to convert from Kelvin to Degrees Celsius.

### 2.2.2. TRMM 3B43 Precipitation Product

Monthly precipitation data from the TRMM 3B43 product, from January to December for the years 2013-2022, was downloaded from <http://reverb.echo.nasa.gov>, to calculate the monthly average rainfall in the Nan Watershed, Northern Thailand.

### 2.2.3. Rainfall Data

Daily rainfall data was collected from the Upper Northern Region Irrigation Hydrology Center, Thailand in the five provinces within the Nan Watershed, Northern Thailand, over a 10-year period (2013-2022) from seven stations. The data included details such as province, period, station name, station code, and rainfall amount. The annual accumulated rainfall average and the maximum and minimum rainfall were calculated to observe the correlation and variability of rainfall, whether increasing or decreasing.

## 2.3. Methodology

### 2.3.1. Normalized Monthly Precipitation Anomaly Percentage (PA)

This measures the deviation of rainfall from the average over a specified period and can be analyzed using Equations 1 and 2 (Shao-E & Bing-Fang, 2010).

$$PA = \frac{P - \bar{P}}{\bar{P}} * 100\% \quad (1)$$

The current precipitation, denoted as P, and the mean precipitation during the same period, denoted as  $\bar{P}$ , are used to calculate the Precipitation Anomaly (PA). This PA can be utilized to assess drought conditions based on the deviation from the average rainfall. The PA values may be either positive or negative. An alternative approach is to derive a Monthly Precipitation Anomaly Percentage (NPA) with values ranging from 0 to 1 using the Equation 2.

$$NPA = \frac{PA - PA_{\min}}{PA_{\max} - PA_{\min}} \quad (2)$$

The minimum and maximum values of the NPA are denoted as  $PA_{\min}$  and  $PA_{\max}$ , respectively.

### 2.3.2 Vegetation Health Index (VHI)

VHI considers the biophysical and climatic conditions of the local area and can be used to monitor actual plant drought in different agrometeorological regions. The basic principle of VHI is that low NDVI and high LST indicate poor plant health. VHI can be analyzed using Equations 3-5 (Kogan, 1998).

$$VCI = \frac{NDVI - NDVI_{\min}}{NDVI_{\max} - NDVI_{\min}} \quad (3)$$

$$TCI = \frac{LST - LST_{\min}}{LST_{\max} - LST_{\min}} \quad (4)$$

$$VHI = a * VCI + b * TCI \quad (5)$$

$NDVI_{\min}$  and  $NDVI_{\max}$  represent the minimum and maximum values of NDVI, while  $LST_{\min}$  and  $LST_{\max}$  represent the minimum and maximum values of LST. The weight coefficients of VCI and TCI are denoted as a and b. Given the current lack of knowledge regarding the contribution of moisture and temperature during the vegetation cycle, it is assumed that the share of VCI and TCI is equal ( $a = b = 0.5$ ). The VHI for the study area was calculated from January to December over the entire period from 2001 to 2014.

2.3.3. Normalized Vegetation Supply Water Index (NVSWI)

During periods of drought, plants close their stomata to conserve water, which in turn reduces transpiration as leaf surface temperature (LST) rises. This phenomenon is evident in smaller plants as a result of lower soil evaporation. Equations 6-7 can be utilized to analyze NVSWI (Carlson et al., 1994).

$$VSWI = \frac{NDVI}{LST} \tag{6}$$

The VSWI is limited to representing relative spatial location and cannot be compared over time series. Therefore, the NVSWI was introduced, calculated using the formula provided by Abbas et al., (2014).

$$NVSWI = \frac{VSWI - VSWI_{\min}}{VSWI_{\max} - VSWI_{\min}} \tag{7}$$

VSWI<sub>min</sub> and VSWI<sub>max</sub> represent the minimum and maximum values of VSWI for the pixel over the study period. The NVSWI for the Nan Watershed from January to December for the entire period of 2012-2022 was computed.

2.4. Correlation and Simple Linear Regression Analysis

This involves Correlation (Equations 8) and Simple Linear Regression Analysis (Equations 9) between the TRMM 3B43 product and ground-based rainfall data and the three types of droughts indices.

$$r = \frac{\sum (x_i - \bar{x})(y_i - \bar{y})}{\sqrt{\sum (x_i - \bar{x})^2 \sum (y_i - \bar{y})^2}} \tag{8}$$

$r$  represents the correlation coefficient.  $x_i$  denotes the values of the x-variable within a sample.  $\bar{x}$  signifies the average of the x-variable values.  $y_i$  indicates the values of the y-variable in a sample, while  $\bar{y}$  represents the mean of the y-variable values.

$$y = ax + b \tag{9}$$

In this context, Y signifies the dependent variable, a indicates the slope of the regression equation, X refers to the independent variable, and b represents a constant term.

3. RESULTS AND DISCUSSION

3.1. NDVI and LST Analysis Results

The analysis results of NDVI are shown in **Table 1**, which presents the NDVI values in the Nan Watershed. **Table 1** indicates that NDVI values are highest in October, with a maximum value of 0.758, and lowest in April, with a value of 0.488. This suggests that NDVI values are high during the rainy season and low during the summer due to insufficient water or drought conditions. The central and lower parts of the Nan Watershed have higher NDVI values due to irrigation water, promoting better plant growth.

Table 1.

## Analysis result of NDVI.

NDVI	2013	2014	2015	2016	2017	2018	2019	2020	2021	2022
Jan	0.593	0.595	0.684	0.626	0.632	0.593	0.593	0.595	0.684	0.632
Feb	0.570	0.543	0.575	0.585	0.627	0.570	0.543	0.543	0.575	0.627
Mar	0.618	0.532	0.516	0.620	0.581	0.618	0.635	0.532	0.516	0.581
Apr	0.565	0.494	0.488	0.657	0.715	0.565	0.596	0.494	0.488	0.715
May	0.553	0.628	0.516	0.691	0.634	0.553	0.632	0.628	0.516	0.634
Jun	0.687	0.737	0.575	0.687	0.554	0.687	0.687	0.737	0.575	0.554
Jul	0.698	0.752	0.691	0.748	0.590	0.698	0.654	0.752	0.691	0.590
Aug	0.717	0.723	0.739	0.767	0.751	0.717	0.654	0.753	0.739	0.751
Sept	0.705	0.750	0.729	0.675	0.752	0.705	0.659	0.750	0.729	0.752
Oct	0.694	0.746	0.758	0.714	0.664	0.694	0.657	0.746	0.748	0.697
Nov	0.693	0.698	0.688	0.688	0.697	0.693	0.752	0.698	0.688	0.697
Dec	0.632	0.616	0.631	0.645	0.706	0.632	0.658	0.616	0.631	0.706

In contrast, the upper part of the basin, which is mountainous and far from irrigation sources, shows lower NDVI values. **Fig.2(a)** illustrates that the upper basin, shown in yellow to orange (low NDVI), and the lower basin, shown in green (high NDVI), do not face severe drought due to irrigation water mitigating drought effects. LST analysis results are presented in **Table 2** and **Fig.2(b)**.

Table 2.

## Analysis result of LST.

NDVI	2013	2014	2015	2016	2017	2018	2019	2020	2021	2022
Jan	27.55	27.55	26.54	28.37	27.98	27.60	26.33	28.56	27.60	28.52
Feb	30.69	30.69	30.27	29.38	30.72	31.17	30.65	29.08	31.17	29.08
Mar	32.76	32.76	33.61	34.65	33.69	33.49	32.64	32.62	33.49	32.63
Apr	33.75	33.75	34.77	38.29	34.62	36.73	33.87	34.61	36.73	32.65
May	34.33	34.33	34.99	36.99	33.30	33.59	32.61	32.59	33.21	29.77
Jun	29.56	29.56	32.71	31.33	29.76	29.56	27.36	29.77	31.01	28.37
Jul	28.96	28.96	29.39	28.62	28.42	28.62	28.36	28.37	29.13	28.25
Aug	27.45	27.45	28.73	29.13	28.19	27.54	28.77	28.25	27.24	28.06
Sept	27.43	27.43	28.39	26.72	28.37	27.43	27.70	28.06	26.51	27.62
Oct	28.49	28.49	28.41	27.77	27.50	28.65	27.63	27.62	27.16	27.36
Nov	28.42	28.42	27.88	28.28	27.37	28.64	27.66	25.49	27.63	25.49
Dec	27.92	24.65	27.18	27.68	26.49	27.99	27.65	27.36	26.69	26.12

**Figure 2(b)** shows that the central and lower parts of the Nan Watershed, being urban areas, have moderate to high LST values (yellow to red), caused by heat emissions from human activities. The upper part, being mostly mountainous and forested, has low LST values. **Table 2** shows that LST is highest in April (summer), reaching 36.73°C, and lowest in December at 24.65°C.

### 3.2. Verification of TRMM 3B42 Product with Ground Station Data

The accuracy verification of the TRMM 3B42 product with ground-based rainfall data in this study is shown in **Fig. 3**. The **figure 3** shows a high correlation between TRMM 3B42 data and ground-based rainfall data, with a correlation coefficient of 0.894. Therefore, the TRMM 3B42 product can be used to determine rainfall patterns in the Nan Watershed.

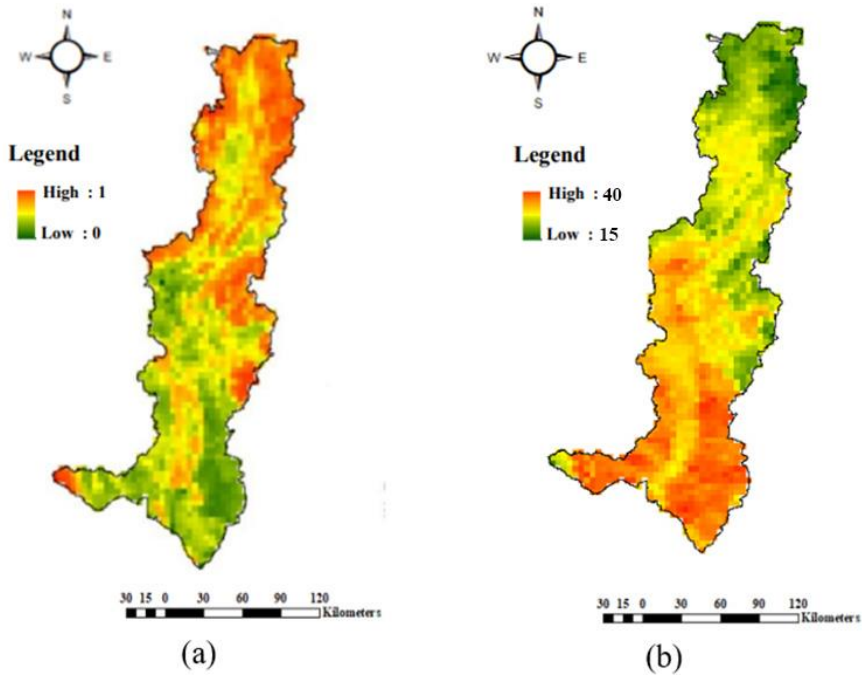


Fig. 2. (a) NDVI and (b) LST.

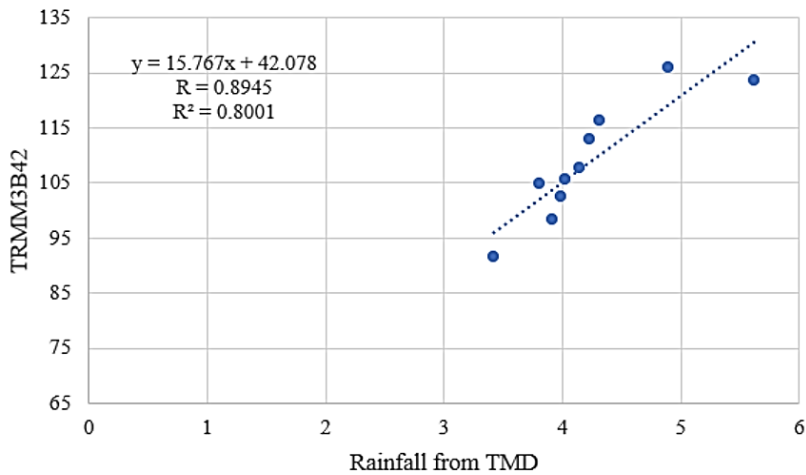


Fig. 3. Correlation between TRMM 3B42 data and ground-based rainfall data.

### 3.3. Evaluation of Suitable Drought Indices

To select the most appropriate index for the Nan Watershed, the indices used in this study (NPA, VHI, and NVSWI) were evaluated for correlation using the TRMM 3B42 product. To assess the suitability of drought indices for evaluating agricultural drought risk in high areas, the study categorized drought levels into five levels, as shown in **Table 3**. The suitable drought index was determined by comparing each calculated index to the criteria, then analyzing the correlation of the three indices with the TRMM 3B42 product.

**Table 3.****Drought levels into five levels.**

Degree of Drought	level of drought
0 - 0.20	Severe drought
0.21 – 0.40	Moderate drought
0.41 – 0.60	Low drought
0.61 – 0.80	Normal
0.81 - 1	Humid

- **NPA Index:** This index calculates the monthly deviation percentage of rainfall, using rainfall data from ground stations in the Nan Watershed, as shown in **Table 4**. **Table 4** indicates that NPA values are relatively low from January to March, increase from April to September, and then decrease until December (maximum NPA value of 1 and minimum of 0). The highest NPA values occur in June and July. The average NPA index from 2013-2022 shows low values in 2013-2014, an increase in 2015, and little variation in subsequent years, with a maximum value of 1.000 in 2016 and a minimum of 0.000 in 2013. A limitation of this index is its inability to assess spatial distribution, as NPA only considers rainfall, causing some monthly discrepancies in analysis results. Despite this, a statistical correlation analysis between TRMM 3B42 and NPA shows a high correlation, with a coefficient of 0.867, indicating a strong relationship between the two variables.

**Table 4.****Exhibits the mean value of the NPA index.**

NPA	2013	2014	2015	2016	2017	2018	2019	2020	2021	2022
<b>Jan</b>	0	0.512	1	0.569	0	0	0.011	0.194	0.633	0
<b>Feb</b>	0.201	1	0.032	0.009	0	0.110	0.845	0	0.379	0.110
<b>Mar</b>	0.147	0.246	0.016	0.199	0	0.084	1	0.176	0.019	0.084
<b>Apr</b>	0.612	0.692	0.529	0	1	0.204	0.194	0.578	0.194	0.265
<b>May</b>	0.368	0.398	0.264	0.588	1	0.068	0.184	0.599	0	0.596
<b>Jun</b>	0.981	0.656	0.292	1	0.839	0.138	0.471	0.298	0.138	0.194
<b>Jul</b>	0.560	0.482	0.351	0.687	1	0.205	0.510	0.766	0.205	0.184
<b>Aug</b>	0.429	0.753	0.292	1	0.860	0.307	0.387	0.387	0.307	0.068
<b>Sept</b>	0.707	0.316	0.267	0.311	0.626	0.005	1	0.984	0.005	0.766
<b>Oct</b>	0.416	0.364	0.401	0.571	0	0.220	1	0.158	0.220	0.17
<b>Nov</b>	0.546	0.341	0.679	0.459	0.133	0.006	0	0.442	0.006	1
<b>Dec</b>	0.362	0.003	0.435	0.001	0	0	1	0.041	0.003	0

- **VHI Index:** The VHI Index is calculated by analyzing NDVI and LST data to create a drought monitoring index that reflects normal NDVI conditions. According to the VHI analysis results presented in **Table 5**, the highest VHI values are observed in March and November, reaching a value of 1, while the lowest values are recorded in January, with a value of 0.027. The VHI generally shows an increasing trend over the years, except for 2013 and 2016 when low values were observed. A statistical correlation analysis between TRMM 3B42 and VHI indicates a strong inverse correlation, with a coefficient of -0.8179. This study highlights significant monthly variations in NDVI and LST, leading to an overestimation of drought severity in the analysis results.

- **NVSWI Index:** This index factors in plant transpiration affected by changes in LST. As LST increases, plant stomata close to conserve water, reducing transpiration. NVSWI analysis results (**Table 6**) show the highest value of 0.031 in October 2016 and the lowest of 0.020 in February 2015. The average NVSWI index from 2013-2022 shows little yearly variation. Spatial analysis divides the basin into three parts: the upper basin, being high and natural, faces more severe drought due to lack of irrigation; the central basin, between natural and irrigated areas, faces moderate drought; and the



lower basin, mostly irrigated, faces minimal drought impacts due to irrigation water. A statistical correlation analysis between TRMM 3B42 and NVSWI shows a high correlation, with a coefficient of 0.956.

**Table 5.**

**Exhibits the mean value of the VHI index.**

VHI	2013	2014	2015	2016	2017	2018	2019	2020	2021	2022
Jan	0.315	0.728	0.047	0.662	0.877	0.517	0.726	0.222	0.027	0.475
Feb	0.885	0.655	0.417	0.123	0.614	0.136	0.664	0.331	0.416	0.707
Mar	0.585	0.399	0.416	1.000	0.654	0.625	0.393	0.408	0.356	0.532
Apr	0.455	0.515	0.370	0.500	0.458	0.488	0.522	0.405	0.299	0.865
May	0.533	0.348	0.682	0.622	0.584	0.395	0.578	0.500	0.558	0.756
Jun	0.379	0.578	0.519	0.514	0.609	0.533	0.557	0.389	0.500	0.239
Jul	0.588	0.877	0.495	0.486	0.559	0.499	0.812	0.692	0.500	0.237
Aug	0.467	0.574	0.379	0.997	0.350	0.487	0.844	0.673	0.764	0.581
Sept	0.578	0.413	0.734	0.500	0.755	0.493	0.465	0.176	0.914	0.589
Oct	0.839	0.804	0.883	0.817	0.530	0.377	0.426	0.426	0.561	0.500
Nov	1.000	0.461	0.725	0.696	0.769	0.056	0.236	0.365	0.492	0.605
Dec	0.681	0.072	0.886	0.661	0.532	0.333	0.361	0.395	0.399	0.457

**Table 6.**

**Exhibits the mean value of the NVSWI index.**

NVSWI	2013	2014	2015	2016	2017	2018	2019	2020	2021	2022
Jan	0.022	0.028	0.023	0.024	0.027	0.023	0.024	0.028	0.023	0.023
Feb	0.022	0.021	0.002	0.019	0.020	0.017	0.020	0.018	0.022	0.017
Mar	0.019	0.016	0.016	0.021	0.018	0.017	0.021	0.016	0.017	0.017
Apr	0.018	0.015	0.014	0.010	0.016	0.016	0.023	0.013	0.025	0.014
May	0.017	0.011	0.018	0.013	0.019	0.014	0.024	0.015	0.019	0.020
Jun	0.022	0.021	0.017	0.020	0.024	0.017	0.026	0.017	0.016	0.026
Jul	0.025	0.024	0.023	0.024	0.023	0.023	0.028	0.026	0.018	0.027
Aug	0.026	0.026	0.022	0.026	0.024	0.024	0.026	0.028	0.027	0.027
Sept	0.029	0.026	0.025	0.028	0.026	0.024	0.022	0.023	0.022	0.025
Oct	0.028	0.028	0.027	0.031	0.027	0.024	0.026	0.026	0.024	0.023
Nov	0.027	0.025	0.025	0.025	0.027	0.028	0.025	0.025	0.024	0.024
Dec	0.023	0.026	0.025	0.024	0.026	0.025	0.025	0.025	0.026	0.018

#### 4. CONCLUSIONS

The growth of crops, global food prices, and political unrest are all influenced by drought. The upper Nan Watershed faces severe drought due to mountainous terrain and distance from irrigation, while the central and lower basin areas experience less severe drought due to irrigation. The highest drought occurred in 2013, with the lowest in 2015. Annual droughts are normal, with severity depending on rainfall and climatic variability. The Nan Watershed shows an increasing drought trend. This study aims to evaluate suitable drought indices for assessing agricultural drought risk in highland regions, focusing on the Nan Watershed in Northern Thailand. The analysis of three drought indices (NPA, VHI, and NVSWI) with the TRMM 3B42 product finds NVSWI to have the highest correlation (0.956), indicating its suitability for monitoring agricultural drought in high area highland regions of the Nan Watershed.

## ACKNOWLEDGMENTS

This research project was financially supported by Mahasarakham University.

## REFERENCES

- Abbas, S., Nichol, J.E., Qamer, F.M., & Xu, J. (2014). Characterization of drought development through remote sensing: A case study in central Yunnan, China. *Remote Sensing*, 6(6), 4998–5018. DOI: 10.3390/rs6064998
- Burgan, R.E., R.A. Hartford, & J.C. Eidenshink. (1996). Using NDVI to Assess Departure from Average Greenness and Its Relation to Fire Business, Gen. Tech. Rep. INT-GTR-333, U.S. Department of Agriculture, Forest Service, Intermountain Research Station, Ogden, Utah, 8 p.
- Carlson, T. N., Gillies, R. R., & Perry, E. M. (1994). A method to make use of thermal infrared temperature and NDVI measurements to infer surface soil water content and fractional vegetation cover. *Remote Sensing Reviews*, 9(1–2), 161–173. DOI: 10.1080/02757259409532220
- Chen, S., Zhong, W., Pan, S., Xie, Q., & Kim, T. W. (2020). Comprehensive drought assessment using a modified composite drought index: A case study in Hubei Province, China. *Water*, 12(2), 462. DOI: 10.3390/w12020462
- Copernicus. (2020). OBSERVER: What impact does drought have on vegetation, and how does Copernicus help? Available online: <https://www.copernicus.eu/en/news/news/observer-what-impact-does-drought-have-vegetation-and-how-does-copernicus-help> (Accessed on 20 March 2024)
- Cui, A., Li, J., Zhou, Q., Zhu, R., Liu, H., Wu, G., & Li, Q. (2021). Use of a multiscalar GRACE-based standardized terrestrial water storage index for assessing global hydrological droughts. *Journal of Hydrology*, 603, p.126871. DOI: 10.1016/j.jhydrol.2021.126871
- Fussel, H. M., & Klein, R. J. T. (2006). Climate change vulnerability assessments: An evolution of conceptual thinking. *Climatic Change*, 75(3), 301–329. DOI: 10.1007/s10584-006-0329-3
- Haidu, I., & Magyari-Saska, Z. (2010). Drought and Extreme Moisture in Small Mountainous Basins. *Geographia Technica*, 5(2), 51–58.
- Hannaford, M. J. (2018). Long-term drivers of vulnerability and resilience to drought in the ZambeziSave area of southern Africa, 1505–1830. *Global and planetary change*, 166, 94–106. DOI: 10.1016/j.gloplacha.2018.05.001
- Hongthong, A., & Nakapan, S. (2023). Assessing the impact of a waste incinerator on the environment using the MAIAC-AOD and AERMOD models. *Frontiers in Environmental Science*, 11, 1240705.
- Iamampai, S., Kanasut, J., Kantawong, B., & Rangsiwanichpong, P. (2023). Drought Hazard Assessment Using Anomaly Drought Index and Geographic Information System in The Chi River Basin, Thailand. *Geographia Technica*, 18(1), 39–55. DOI: 10.21163/GT\_2023.181.04
- Itsarawisut, J., Puckdeevongs, A., & Laosuwan, T. (2024). Environmental Monitoring on the Surface of The Andaman Sea Over the Southwestern Coast of Thailand: A Case Study of Spatial and Temporal Variability of Chlorophyll-A. *Geographia Technica*, 19(2), 57–69. DOI: 10.21163/GT\_2024.192.05
- Kamanga, T.F., Tantanee, S., Mwale, F.D., & Buranajarukorn, P. (2020). A Multi Hazard Perspective in Flood and Drought Vulnerability: Case Study of Malawi. *Geographia Technica*, 15(1), 132–142. DOI: 10.21163/GT\_2020.151.12
- Kogan, N. (1990). Personality and aging. In J. E. Birren & K. W. Schaie (Eds.), *Handbook of the psychology of aging* (3rd ed., pp. 330–346). Academic Press. DOI: 10.1016/B978-0-12-101280-9.50026-7
- Kogan, F.N. (1998). Global drought and flood-watch from NOAA polar-orbiting satellites. *Adv. Space Res.* 21 (3), 477–480.

- Laosuwan, T., Uttaruk, Y., & Rotjanakusol, T. (2022). Analysis of Content and Distribution of Chlorophyll-a on the Sea Surface through Data from Aqua/MODIS Satellite. *Polish Journal of Environmental Studies*, 31(5), 4711-4719. <https://doi.org/10.15244/pjoes/150731>
- Lloyd-Hughes, B., & Saunders, M.A. (2002). A drought climatology for Europe. *International Journal of Climatology*, 22(13), 1571–1592. DOI: 10.1002/joc.846
- Li, H., Yin, Y., Zhou, J., & Li, F. (2024). Improved Agricultural Drought Monitoring with an Integrated Drought Condition Index in Xinjiang, China. *Water*, 16(2),325. DOI: 10.3390/w16020325
- Liu, W., Ma, S., Feng, K., Gong, Y., Liang, L., & Tsubo, M. (2023). The Suitability Assessment of Agricultural Drought Monitoring Indices: A Case Study in Inland River Basin, *Agronomy*, 13(2), 469. DOI: 10.3390/agronomy13020469
- Magyari-Saska, Z. & Haidu, I., (2009). Drought and Extreme Moisture Evaluation and Prediction with GIS Software Module. In *Proceedings of the ITI 2009, 31st International Conference on Information Technology Interfaces* (editors: LuzarStiffler, V; Jarec, I; Bekic, Z.), page 553-+, Univ Zagreb & IEEE Reg 8, DOI:10.1109/ITI.2009.5196146.
- Meena, P., & Laosuwan, T. (2021). Spatiotemporal Variation Analysis of Atmospheric Carbon Dioxide Concentration using Remote Sensing Technology. *International Journal on Technical and Physical Problems of Engineering*, 13 (3), 7-13.
- Ministry of Natural Resources and Environment. (2011). Nan Watershed. Available online: [http://lib.mnre.go.th/lib/report/reo3\\_54.pdf](http://lib.mnre.go.th/lib/report/reo3_54.pdf) (Accessed on 28 March 2024)
- Muyambo, F., Jordaan, A. J., & Bahta, Y. T. (2017). Assessing social vulnerability to drought in South Africa: Policy implication for drought risk reduction. *Jambá: Journal of Disaster Risk Studies*, 9(1), 1-7.
- Nakapan, S., & Hongthong, A. (2022). Applying surface reflectance to investigate the spatial and temporal distribution of PM2.5 in Northern Thailand. *ScienceAsia*, 48, 75-81.
- Nanzad, L., Zhang, J., Tuvdendorj, B., Nabil, M., Zhang, S., & Bai, Y. (2019). NDVI anomaly for drought monitoring and its correlation with climate factors over Mongolia from 2000 to 2016. *Journal of arid environments*. 164, 69-77. DOI: 10.1016/j.jaridenv.2019.01.019
- Ndayiragije, J.M., & Li, F. (2022). Effectiveness of Drought Indices in the Assessment of Different Types of Droughts, Managing and Mitigating Their Effects. *Climate*, 10(9), 125. DOI: 10.3390/cli10090125
- Prabnakorn, S., Maskey, S., Suryadi, F. X., & de Fraiture, C. (2018) Rice yield in response to climate trends and drought index in the Mun River Basin, Thailand. *Science of the Total Environment*. 621, 108-119. DOI: 10.1016/j.scitotenv.2017.11.136
- Raksapatcharawong, M., Veerakachen, W., Homma, K., Maki, M., & Oki, K. (2020). Satellite-based drought impact assessment on rice yield in Thailand with SIMRIW– RS. *Remote Sensing*. 12(13), p. 2099. DOI: 10.3390/rs12132099
- Rotjanakusol, T., & Laosuwan, T. (2018). Remote Sensing Based Drought Monitoring in The Middle-Part of Northeast Region of Thailand. *Studia Universitatis Vasile Goldis: Seria Stiintele Vietii*, 28(1), 14-21.
- Rotjanakusol, T., & Laosuwan, T. (2019). Drought Evaluation with NDVI-based Standardized Vegetation Index in Lower Northeastern Region of Thailand. *Geographia Technica*, 14(1), 118-130. DOI:10.21163/GT\_2019. 141.09
- Rotjanakusol, T., & Laosuwan, T. (2020). Model of Relationships between Land Surface Temperature and Urban Built-Up Areas in Mueang Buriram District, Thailand. *Polish Journal of Environmental Studies*, 29(5), 3783-3790. DOI: 10.15244/pjoes/116384
- Shao-E, Y., & Bing-Fang, W. (2010). Calculation of monthly precipitation anomaly percentage using web-serviced remote sensing data. *Advanced Computer Control (ICACC)*, 2010 2<sup>nd</sup> International Conference. vol. 5. IEEE, pp. 621–625
- Tucker, C. J., & Sellers, P. (1986). Satellite Remote Sensing of Primary Production. *International Journal of Remote Sensing*, 7, 1395-1416. DOI: 10.1080/01431168608948944

- Rouse, J.W., Haas, R.H., Schell, J.A. & Deering, D.W. (1974). Monitoring Vegetation Systems in the Great Plains with ERTS. Third ERTS-1 Symposium NASA, NASA SP-351, Washington DC, 309-317.
- Unganai, L.S., & Kogan, F.N. (1998). Drought monitoring and corn yield estimation in southern Africa from AVHRR data, *Remote Sensing of Environment*, 63, 219-232.
- Uttarak, Y., & Laosuwan, T. (2019). Drought Analysis Using Satellite-Based Data and Spectral Index in Upper Northeastern Thailand. *Polish Journal of Environmental Studies*, 28(6), 4447-4454. DOI:10.15244/pjoes/94998
- Wang, X., Zhuo, L., Li, C., Engel, B.A. Sun, S., & Wang, Y. (2020). Temporal and spatial evolution trends of drought in northern Shaanxi of China: 1960–2100. *Theoretical and Applied Climatology*, 139(2), 965–979. DOI: 10.1007/s00704-019-03024-2
- Wongtui, B., & Nilsonthi, P. (2024). Analysis of Agricultural Drought Risk Areas and Influencing Factors in the Mae Wang River Basin, Chiang Mai Province. *Life Sciences and Environment Journal*, 25(1), 212–224. DOI: 10.14456/lsej.2024.17
- Wu, X., Xu, H., He, H., Wu, Z, Lu G, Liao T. (2024). Agricultural Drought Monitoring Using an Enhanced Soil Water Deficit Index Derived from Remote Sensing and Model Data Merging. *Remote Sensing*, 16(12),2156. DOI: 10.3390/rs16122156
- Yu, Z., Wang, T., Wang, P., Yu, J. (2022). The Spatiotemporal Response of Vegetation Changes to Precipitation and Soil Moisture in Drylands in the North Temperate Mid-Latitudes. *Remote Sensing*, 14(15), 3511. DOI: 10.3390/rs14153511
- Zargar, A., Sadiq, R., Naser, B., Khan, F.I. (2011). A review of drought indices. *Environmental Reviews*,19, 333–349.
- Zhou, Z.Y., Long, Q.B., Bai, P. (2021). Scale of meteorological drought index suitable for characterizing agricultural drought: A case study of hunan province. *J. South–North Water Transf. Water Sci. Technol*, 19, 119–128.